ELSEVIER

Journal of Alloys and Compounds 300–301 (2000) 261–266

Journal of ALLOYS AND COMPOUNDS

www.elsevier.com/locate/jallcom

Radiative recombination in BaF_2:Pr

W. Drozdowski*, A.J. Wojtowicz

Institute of Physics, Nicholas Copernicus University, Grudziądzka 5/7, 87-100 Toruń, Poland

Abstract

In this communication some preliminary results of studies on radiative recombination processes in praseodymium-doped barium fluoride crystals are reported. Experimental techniques such as measurements of radioluminescence, thermoluminescence, VUV-excited photoluminescence spectra and photoluminescence time profiles at various temperatures are employed. The Pr^{3+} ions can be excited directly or via some kind of host-to-ion energy transfer. The thermoluminescence glow curve is separated into nine first-order peaks, to which the corresponding radiation defects are assigned and activation energies are found. It is shown that one of these defect centers, i.e., the V_K center, influences the luminescence time profiles above 140 K in case of excitation involving the host-to-ion energy transfer.

Keywords: Radiation effects; Recombination; Trapping; Luminescence; Synchrotron radiation

1. Introduction

Barium fluoride is the fastest known inorganic scintillator, first introduced by Farukhi and Swinehart [1]. Its very fast (<1 ns [2,3]), but relatively low-efficient scintillation at about 190 and 220 nm is due to so-called core-to-valence (CV) luminescence [4], also referred to as cross-over (CO) or cross-luminescence [5]. Besides the CV luminescence, under ionizing radiation BaF_2 emits a much stronger broad band peaking at about 300 nm, originating in radiative decay of self-trapped excitons (STE). The presence of this slow (~1 μs [4]) emission is a serious deficiency wherever a short decay time constant is required (e.g., in high energy physics), thus efforts are being made to replace it by doping the BaF_2 host with a suitable rare earth ion characterized by fast and efficient luminescence of its own.

Most of the attention has been focused on cerium-doped barium fluoride, proposed as a substitution for pure BaF_2 by Czirr and Catalano [6]. Extensive studies on recombination processes in BaF_2:Ce have been performed by Visser et al. [7,8]. The influence of charge trapping processes on the scintillation mechanism, first considered for the case of $YAlO_3$:Ce and $LuAlO_3$:Ce [9,10], has also been examined for BaF_2:Ce [11]. Thermoluminescence glow curves below and above room temperature have been measured and interpreted in terms of thermally activated decomposition of defect centers. These curves exhibit a number of peaks, both these reported earlier in literature [12,13] and those previously unknown [11,14,15]. All the defect centers have been found to play an important role in the scintillation process: they are responsible for finite rise times and slow components in the scintillation time profiles as well as for a decreased light yield.

On the contrary to Ce-doped BaF_2, Pr-doped BaF_2 has received much less attention so far. This fact is hardly understandable, as some luminescence properties, particularly the shorter radiative lifetime of Pr^{3+} ions [16], favor BaF_2:Pr. Therefore we have decided to improve the present state of knowledge on radiative recombination in BaF_2:Pr by similar studies as in the case of BaF_2:Ce [11,15]. In this communication we present some initial results of this research.

2. Materials and experiments

The crystal of BaF_2:0.2% Pr was grown by Optovac Inc. (North Brookfield, USA) using the Bridgman method. The praseodymium concentration is that added to the melt (in mole%). No contamination by oxygen was observed and the samples were not subjected to any chemical reducing procedure.

Radioluminescence was measured with a set-up consisting of an X-ray tube operated at 35 kV and 25 mA, a 0.5 m monochromator (SpectraPro-500 made by Acton Research

---

*Corresponding author. Tel.: +48-56-611-3319; fax: +48-56-622-5397.

E-mail address: wind@phys.uni.torun.pl (W. Drozdowski)

0925-8388/00/$ – see front matter © 2000 Published by Elsevier Science S.A. All rights reserved.
PII: S0925-8388(99)00780-X

Corporation) and a photomultiplier (R928 made by Hamamatsu). The spectral resolution was about 1 nm.

Synchrotron radiation excited spectra, thermoluminescence (TL) and time profiles were recorded at the SUPERLUMI station, which is an experimental setup at the high intensity beamline I of HASYLAB, Hamburg, Germany. The sample was mounted in a helium-flow cryostat. Before being focused on the crystal, the synchrotron light went through a 2 m excitation monochromator of vertical McPherson mounting. For luminescence analysis a 0.5 m BM50 Czerny-Turner monochromator with a Hamamatsu R2059 photomultiplier was used. The spectral resolution was 0.4 and 6.4 nm in the excitation and luminescence channels, respectively. Sodium salicylate was used to examine the wavelength dependence of the synchrotron radiation intensity. The correction curve obtained in this way was used to correct the excitation spectra.

Prior to the TL-run the sample was irradiated for 30 min with white synchrotron light (the excitation monochromator was set to the 0th order) at liquid helium temperature. Subsequently the helium flow was closed and the temperature inside the cryostat began to increase. An approximately constant heating rate of 0.044 K/s was achieved using a heater connected with a temperature controller (T3000 by TRI Research). The TL signal was detected by a channel plate (IPDM18 by ITL/Photek) in the spectral range between 230 and 330 nm and then integrated.

A more detailed description of the SUPERLUMI station was given by Zimmerer in Ref. [17].

3. Results and discussion

An X-ray excited luminescence spectrum of BaF_2:Pr is shown in Fig. 1. The spectrum consists of strong Pr^{3+} d–f (i.e., $4f5d$–$4f^2$) lines between 222 and 280 nm, imposed on the CV (~220 nm, hardly resolvable) and excitonic (~250–450 nm) luminescence bands. In addition, Pr^{3+} f–f emission occurs above 450 nm. As the d–f lines are higher in energy than the STE band, an energy transfer from the excitons to the Pr^{3+} ions, known from BaF_2:Ce [7,8], is rather excluded and thus the d–f luminescence must be excited by consecutive capture and recombination of charge carriers generated by ionizing radiation. To assign the d–f and f–f lines to transitions between definite electronic states, we took the energies of the Pr^{3+} $4f^2$ multiplets from the paper of Hargreaves [18] and assumed after Loh [19] that the lowest $4f5d$ state is located 45 600 cm^{-1} above the lowest $4f^2$ one. Although the data in Refs. [18,19] concern CaF_2:Pr, the calculated emission wavelengths agree well with the experimental ones (see Table 1 for details).

Representative excitation spectra of the aforementioned emissions are presented in Fig. 2. The peaks at 129 and 144 nm (upper and middle window) are characteristic of the STE luminescence (a corresponding spectrum of undoped BaF_2 is almost identical). Some kinks (e.g., at 125 nm) may be artificial, reproducing the reflection properties of BaF_2 crystals reported by Rubloff [20]. The next two bands at 155–175 and 190–220 nm (middle window) are associated with the direct f–d excitation of

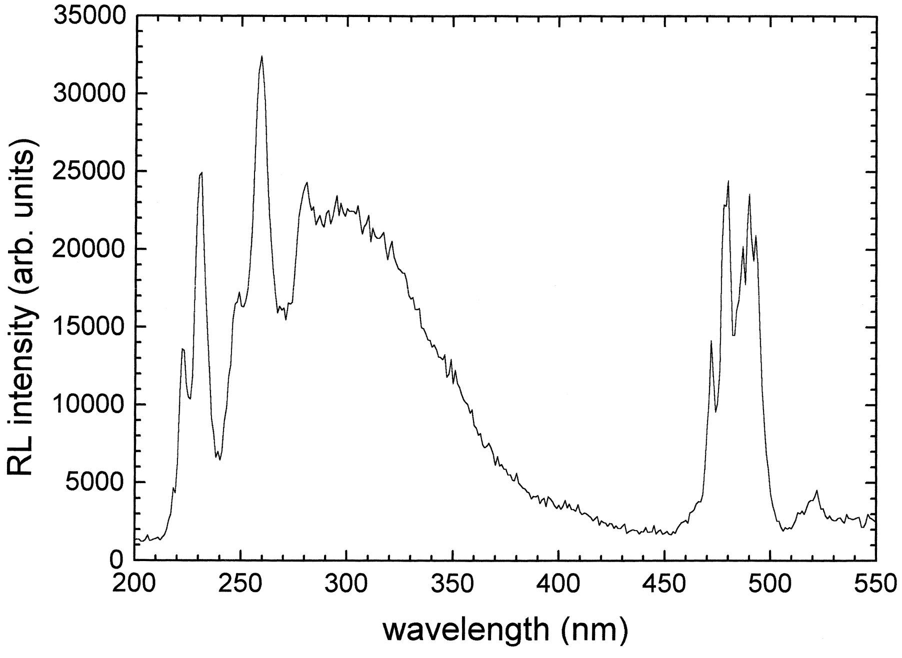

Fig. 1. The X-ray excited emission spectrum of BaF_2:Pr.

Table 1
The maxima of the luminescence lines and bands in Pr-doped CaF_2 and BaF_2 between 200 and 550 nm[a]

Electronic states		Emission wavelength (nm)	
Initial	Final	Calculated (CaF_2)	Experimental (BaF_2)
Lowest $4f5d$	$4f^2\ ^3H_4$	221	222
Lowest $4f5d$	$4f^2\ ^3H_5$	231	231
Lowest $4f5d$	$4f^2\ ^3H_6$	244	249
Lowest $4f5d$	$4f^2\ ^3F_2$	248	249
Lowest $4f5d$	$4f^2\ ^3F_3$	256	259
Lowest $4f5d$	$4f^2\ ^3F_4$	260	259
Lowest $4f5d$	$4f^2\ ^1G_4$	283	280
Lowest $4f5d$	$4f^2\ ^1D_2$	350	350*
Lowest $4f5d$	$4f^2\ ^3P_0$	397	–
Lowest $4f5d$	$4f^2\ ^3P_1$	407	407*
Lowest $4f5d$	$4f^2\ ^1I_6$	412	407*
Lowest $4f5d$	$4f^2\ ^3P_2$	430	438*
$4f^2\ ^3P_2$	$4f^2\ ^3H_4$	451	–
$4f^2\ ^1I_6$	$4f^2\ ^3H_4$	473	472
$4f^2\ ^3P_1$	$4f^2\ ^3H_4$	480	480
$4f^2\ ^3P_0$	$4f^2\ ^3H_4$	494	490
$4f^2\ ^3P_2$	$4f^2\ ^3H_5$	499	–
$4f^2\ ^1I_6$	$4f^2\ ^3H_5$	526	522
$4f^2\ ^3P_1$	$4f^2\ ^3H_5$	534	–

[a] Wavelengths marked by asterisks are taken from the synchrotron radiation excited spectra of much lower resolution than that of the radioluminescence spectrum; the undetected ultraviolet f–f transitions from the highest $4f^2$ state $^1S_0$ are omitted.

the Pr^{3+} ions. Interestingly, the prominent peak in the excitation spectra of the f–f emission (lower window) lies higher in energy than the f–d excitation bands. Similar peaks were observed by Yang and DeLuca [21] in case of the Nd^{3+}, Er^{3+}, and Tm^{3+} ions in trifluorides. Following their explanation we expect an efficient energy transfer from the host to the Pr^{3+} ions, accompanied by a large energy loss not allowing the $4f5d$ levels to be excited. This energy loss can be due to the lattice relaxation via formation of self-trapped hole centers, known as the V_K centers. Above 230 nm all the excitation spectra reveal no important features. Although the band at 290 nm could suggest an unintended cerium impurity, it is more probably caused by the 2nd order of the grating of the emission monochromator.

Fig. 3 shows emission spectra taken under selective synchrotron radiation excitation (note lower resolution than in radioluminescence measurements). In agreement with expectations, the STE band dominates at 120 nm, the Pr^{3+} d–f luminescence at 200 nm, and the Pr^{3+} f–f luminescence at 135 nm excitation. Besides the emissions observed in radioluminescence, some bands that are unresolvable therein occur at 350, 407, and 438 nm. They are associated with the Pr^{3+} d–f transitions, what is confirmed

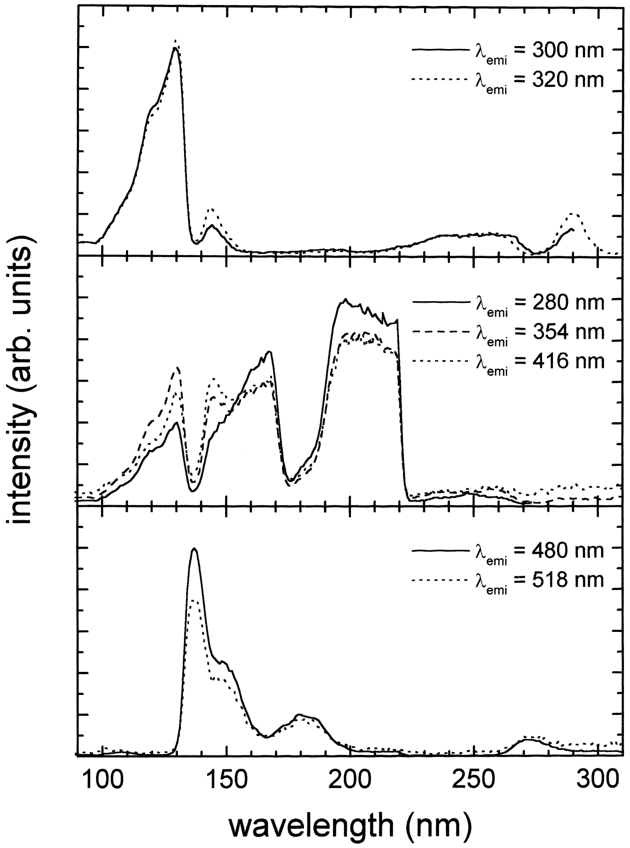

Fig. 2. The excitation spectra of selected emissions in BaF_2:Pr.

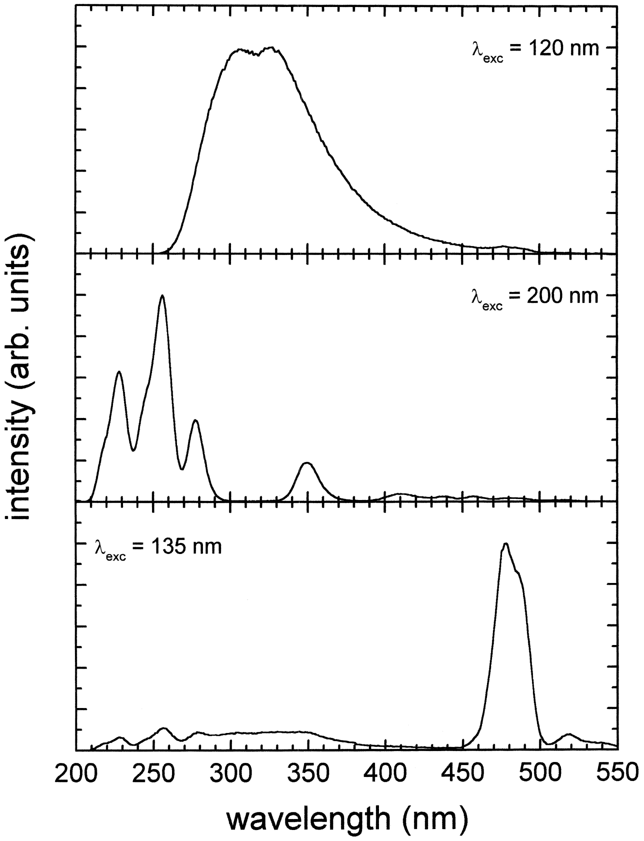

Fig. 3. The synchrotron radiation excited emission spectra of BaF_2:Pr.

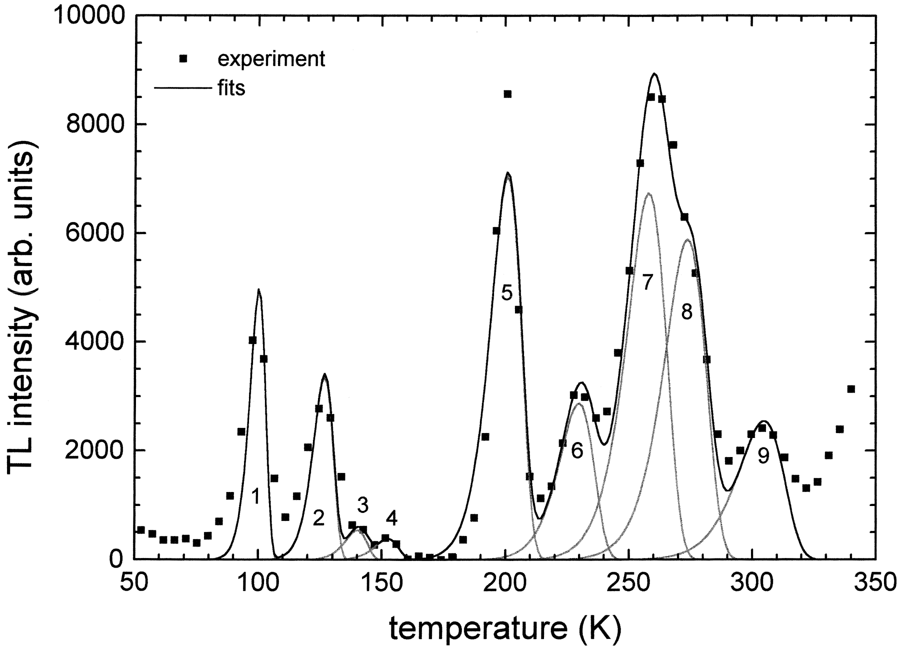

Fig. 4. The glow curve of BaF_2:Pr measured at a heating rate of 0.044 K/s.

both by excitation spectra (middle window of Fig. 2) and calculations (Table 1).

A glow curve of BaF_2:Pr is presented in Fig. 4. In spite of its composite structure, characteristic asymmetry of the major peaks is visible. This fact suggests that the simple TL model of Randall and Wilkins [22] may be used to analyze the data. Indeed, we achieved satisfactory results in separating the curve into nine first-order peaks (Fig. 4). This was done by fitting the following expression (based on the Randall–Wilkins formula) to experimental points:

$$I(T)=\sum_{i=1}^{9} n_{0i} s \exp\left(-\frac{E_i}{k_\mathrm{B} T}\right) \times \exp\left(-\frac{s}{\beta}\int_{T_0}^{T}\exp\left(-\frac{E_i}{k_\mathrm{B} T'}\right)\mathrm{d}T'\right) \qquad (1)$$

(I denotes the TL intensity; T, the temperature; β, the heating rate; n_0, the initial concentration of defect centers; E, the activation energy; s, the frequency factor; and k_B, the Boltzmann constant). Preliminary input values of n_{0i} and E_i for the fitting procedure were chosen by trial and error, while the frequency factor was fixed at $s=4.23\times 10^{11}$ s ($\ln s=26.77$) after Wojtowicz et al. [15]. The results, summarized in Table 2, are rather not affected by a non-ideal heat transfer, as the heating rate we used (0.044 K/s) is low enough to neglect such an effect. The presence of a number of peaks in glow curves of undoped and rare-earth doped alkaline-earth fluorides irradiated at low temperature was attributed to thermal activation of motion of radiation-induced defect centers by Merz and Pershan [23]. Although one could expect quite similar curves regardless of the rare-earth doping, there are remarkable differences among those reported in the literature [12,13,15,24]. Only the first peak always occurs at about 100 K and is generally accepted to be related to the V_K centers. Comparing the peak positions and corresponding parameters (Table 2) with the data of Wojtowicz et al. [15], we assign the peaks Nos. 2, 4, 5, and 6 of our curve to the H', H, $V_{\mathrm{KA}'}$, and V_KA centers, respectively. The nature of other centers, which we denote as H'', U_1, U_2, and U_3, is not known, however, they may be associated with Pr^{3+} ions.

In the same temperature range as thermoluminescence (50–350 K), time profiles of the emission detected at 259 nm were recorded. Three excitation wavelengths were selected: 65, 135, and 163 nm. In case of the direct f–d excitation of the Pr^{3+} ions (163 nm) single-exponential decays with decay time constants of about 22 ns, slightly dependent on temperature, were observed, while the set-up

Table 2
Defect centers detected in thermoluminescence of BaF_2:Pr[a]

Peak number	T_max (K)	n_0 (arb. units)	E (eV)	Defect
1	100	9.36×10^5	0.268	V_K
2	127	7.94×10^5	0.342	H'
3	140	1.43×10^5	0.379	H''
4	153	1.10×10^5	0.414	H
5	201	2.60×10^6	0.550	$V_{\mathrm{KA}'}$
6	230	1.21×10^6	0.631	V_KA
7	258	3.17×10^6	0.712	U_1
8	274	2.94×10^6	0.756	U_2
9	305	1.41×10^6	0.844	U_3

[a] T_max = Temperature at peak maximum; n_0 = initial concentration of centers; E = activation energy.

response time was reflected in rise times of about 1 ns. At 65 nm excitation the decay times were even shorter, close to 20.1 ns reported by Pedrini et al. [16]. The prompt emission at core excitation (65 nm) can be explained by the same process that was postulated by Wojtowicz et al. [15,25] for a similar situation in BaF_2:Ce. The 65 nm photons excite the crystal, creating core holes and conduction band electrons of energy too low to separate. This is followed by the CV luminescence leaving behind valence band holes, which may be captured by the Pr^{3+} ions. The resultant Pr^{4+} ions attract conduction band electrons and radiative recombination takes place, producing the fast Pr^{3+} *d–f* luminescence independently of temperature. We remind here that we suggest the same consecutive capture mechanism as responsible for the efficient Pr^{3+} *d–f* emission in radioluminescence.

The most complex profiles, however, were observed at 135 nm excitation (Fig. 5). From 50 to 140 K they resemble those excited at 163 nm, while above 140 K the decay time constants are longer (up to 40 ns). Moreover, above 240 K the rise times are also prolonged (see points in Fig. 6). As shown in Fig. 3. (lower window), the 135 nm excitation gives rise mainly to the Pr^{3+} *f–f* luminescence, but trace amounts of the STE and Pr^{3+} *d–f* luminescences remain. The decay time constants of the STE and Pr^{3+} *f–f* emissions are longer than the synchrotron repetition rate (192 ns), hence they rather contribute only to the background and the decay time of 22 ns dominates until an extra component appears above 140 K. We associate this component with the host-to-ion energy transfer and the lattice relaxation via formation of the V_K centers (discussed earlier). Therefore we expect these centers to introduce their own lifetime to the profiles. Such a lifetime, τ, is a function of the temperature T, the activation energy E, and the frequency factor s, in accordance with the classic Arrhenius formula:

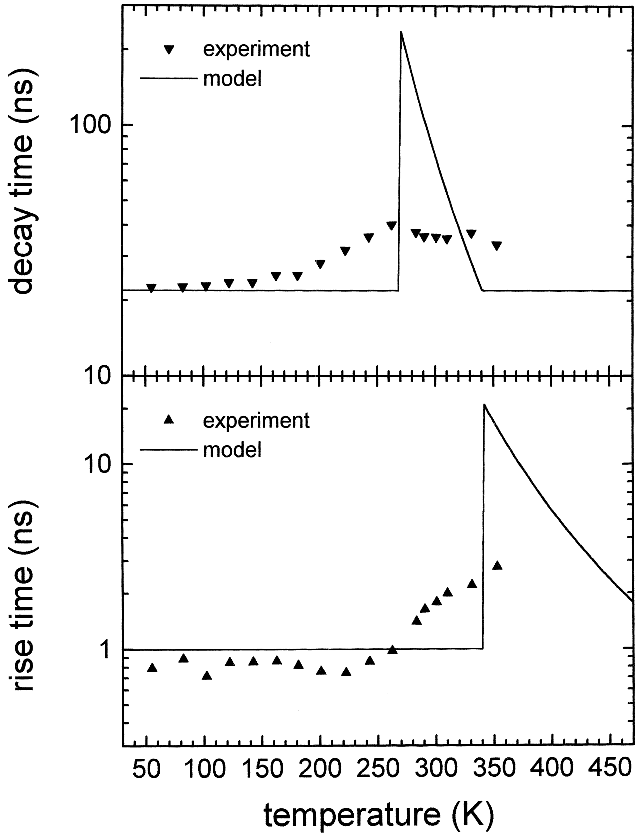

Fig. 6. Decay and rise time constants of the luminescence excited at 135 nm and detected at 259 nm as a function of temperature.

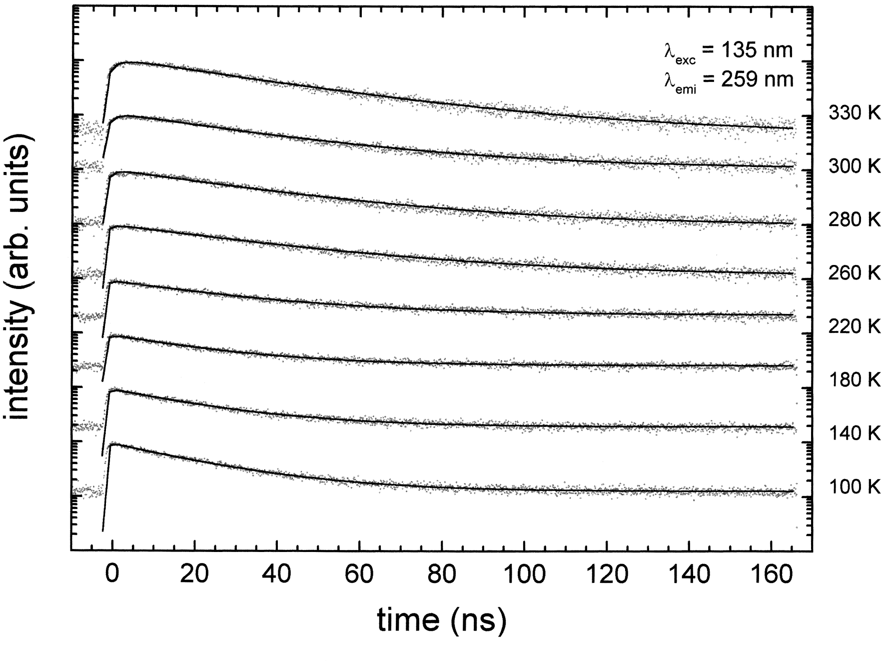

Fig. 5. Representative luminescence time profiles excited at 135 nm and detected at 259 nm at various temperatures.

$$\tau = \frac{1}{s} \exp\left(\frac{E}{k_B T}\right) \quad (2)$$

In a simple model we propose, at low temperatures the lifetimes of the V_K centers are long enough not to contribute to the time profiles and we get the decay times of 22 ns (Pr^{3+} radiative lifetime) and the rise times of 1 ns (instrumental response). For higher temperatures we assume quite arbitrarily that the defect centers influence the decay time constants if $22<\tau<250$ ns, and the rising part of the profiles if $1<\tau<22$ ns. The solid lines in Fig. 6. are plotted according to the model, with the parameters of the V_K center taken from Table 2. Although the model is very simple indeed, it demonstrates reasonably well the relation between the time profiles and the thermal activation of the V_K centers motion. The lifetimes of other defects are too long to contribute to the profiles in the temperature range of our experiments.

4. Conclusions

Our measurements and calculations provide new data on radiative recombination processes in BaF_2:Pr. It is shown that the fast Pr^{3+} d–f luminescence can be excited directly by VUV light as well as by core excitation with VUV light or ionizing radiation. On the contrary, the excitation of the Pr^{3+} f–f luminescence involves a host-to-ion energy transfer and is accompanied by a large energy loss. All these lines and bands are assigned to transitions between appropriate electronic states of the Pr^{3+} ion. The defect centers detected in TL are parametrized and one of them, i.e., the V_K center, is found to affect the luminescence time profiles above 140 K by introducing its own lifetimes. These observations strongly support the contention that the dominant light producing mechanism in the scintillation of BaF_2:Pr is due to consecutive capture and recombination of charge carriers.

Acknowledgements

This work has been supported by the Polish Committee for Scientific Research (2P03B04914), the TMR contract (ERBFMGECT950059) of the European Community, and ALEM Associates, Boston, USA. Hospitality and help of Prof. Georg Zimmerer and Dr. Marco Kirm at HASYLAB is gratefully acknowledged.

References

[1] M.R. Farukhi, C.F. Swinehart, IEEE Trans. Nucl. Sci. NS-18 (1971) 200–204.

[2] M. Laval, M. Moszynski, R. Allemand, E. Cormoreche, P. Guinet, R. Odru, J. Vacher, Nucl. Instr. Meth. 206 (1983) 169–176.

[3] C. Shi, T. Kloiber, G. Zimmerer, J. Lumin. 40/41 (1988) 189–190.

[4] P.A. Rodnyi, Physical Processes in Inorganic Scintillators, CRC Press LLC, New York, 1997.

[5] C.W.E. van Eijk, J. Lumin. 60/61 (1994) 936–941.

[6] J.B. Czirr, E. Catalano, Nucl. Instr. Meth. 143 (1977) 487–488.

[7] R. Visser, P. Dorenbos, C.W.E. van Eijk, A. Meijerink, G. Blasse, H.W. den Hartog, J. Phys.: Condens. Matter 5 (1993) 1659–1680.

[8] R. Visser, J. Andriessen, P. Dorenbos, C.W.E. van Eijk, J. Phys.: Condens. Matter 5 (1993) 5887–5910.

[9] A.J. Wojtowicz, J. Głodo, A. Lempicki, C. Brecher, J. Phys.: Condens. Matter 10 (1998) 8401–8415.

[10] A.J. Wojtowicz, J. Głodo, W. Drozdowski, K.R. Przegiętka, J. Lumin. 79 (1998) 275–291.

[11] J. Głodo, P. Szupryczyński, A.J. Wojtowicz, Acta Phys. Pol. A 95 (1999) 259–268.

[12] A. Tzalmona, P.S. Pershan, Phys. Rev. 182 (1969) 906–913.

[13] J.H. Beaumont, W. Hayes, D.L. Kirk, G.P. Summers, Proc. Roy. Soc. London A315 (1970) 69–97.

[14] W. Drozdowski, K.R. Przegiętka, A.J. Wojtowicz, H.L. Oczkowski, Acta Phys. Pol. A95 (1999) 251–258.

[15] A.J. Wojtowicz, P. Szupryczyński, J. Głodo, W. Drozolowski, D. Wismiewski, Radioluminescence and recombination processes in BaF_2:Ce, J. Phys.: Condensed Matter, submitted.

[16] C. Pedrini, D. Bouttet, C. Dujardin, B. Moine, H. Bill, Chem. Phys. Lett. 220 (1994) 433–436.

[17] G. Zimmerer, Nucl. Instr. Meth. Phys. Res. A308 (1991) 178–186, On-line information: http://www-hasylab.desy.de.

[18] W.A. Hargreaves, Phys. Rev. B6 (1972) 3417–3422.

[19] E. Loh, Phys. Rev. 147 (1966) 332–335.

[20] G.W. Rubloff, Phys. Rev. B5 (1972) 662–684.

[21] K.H. Yang, J.A. DeLuca, Phys. Rev. B17 (1978) 4246–4255.

[22] J.T. Randall, M.H.F. Wilkins, Proc. Roy. Soc. London A184 (1945) 366–407.

[23] J.L. Merz, P.S. Pershan, Phys. Rev. 162 (1967) 217–235.

[24] K. Atobe, J. Chem. Phys. 71 (1979) 2588–2594.

[25] A.J. Wojtowicz, W. Drozdowski, J. Głodo, D. Wiśniewski, HASYLAB Annual Report, HASYLAB, Hamburg, 1998.